5418

12-June-2022

SARS-CoV-2 Omicron And Multi-variant Neutralization Activity Of Ensovibep: A DARPin Therapeutic Candidate For Treatment Of Covid-19

Charles G. Knutson, Novartis Institutes for BioMedical Research, Cambridge, MA, USA

Co-Authors: S. Rothenberger[1], M. Walser[2], F. Malvezzi[2], D. L. Hurdiss[3], J. Mayor[1], H. Moreno[1], S. Ryter[4], N. Liechti[4], A. Bosshart[2], S. Mangold[2], F. Radom[2], K. Ramanathan[5], O. Engler[4], M. T. Stumpp[2]

[1]University of Lausanne, Lausanne, Switzerland; [2]Molecular Partners AG, Zurich-Schlieren, Switzerland; [3]Utrecht University, Utrecht, Netherlands; [4]Spiez Lab., Spiez, Switzerland; [5]Novartis Pharma AG, Basel, Switzerland

Background

- The omicron variant of SARS-CoV-2 has altered the COVID-19 pandemic landscape.
- Omicron's increased transmission and ability to evade natural or vaccine-induced immunity developed against earlier variants is a strong reminder of the power of viral evolution.
- Therapies with potential for multi-variant effectiveness are a key component of effective pandemic management.
- **ENSOVIBEP** is a first-in-class anti-SARS-CoV-2 DARPin (Designed Ankyrin Repeat Protein) therapeutic candidate that uses three distinct DARPin domains (R1, R2, R3) with similar paratopes to cooperatively bind to different regions of the receptor binding domain (RBD) of the SARS-CoV-2 spike protein trimer, thereby preventing interaction with the host ACE2 receptor.
- The multi-specific binding of the RBD binding DARPin modules limits the impact of spike protein mutations on antiviral potency (**Figure 1**).

Figure 1. Global frequencies of point mutations in the spike protein of SARS-CoV-2 according to the GISAID database, including a heat map table with IC_{50} values for ensovibep, R1, R2, R3, for all point mutations tested.

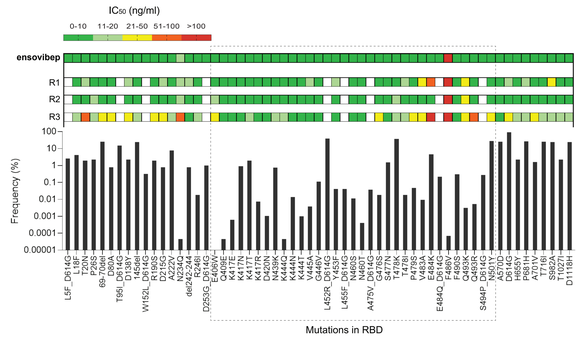

Data from VSV/Lentivirus-based pseudovirus assays; dashed box: mutations in receptor binding domain.

- Depiction based on structural data showing ensovibep RBD binding DARPin domains (green, blue, cyan) binding to the RBD of the SARS-CoV-2 spike protein trimer. The two additional DARPin domains (purple) bind to human serum albumin (HSA, not shown for clarity) to provide half-life extension (**Figure 2**).
- We present here data supporting the multi-variant potency of ensovibep.

Figure 2. Ensovibep bound to the SARS-CoV-2 spike protein.

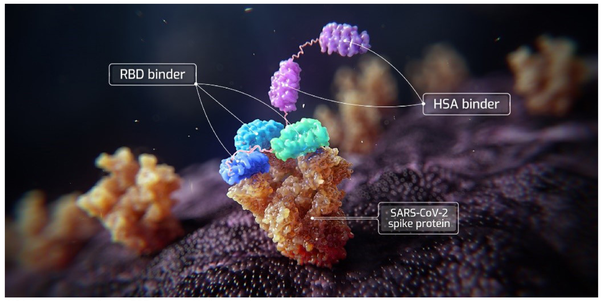

HSA, human serum albumin; RBD, receptor binding domain.

Methods

- The VSV pseudotype viral system (CHUV) was based on the recombinant VSV*DELG-Luc vector in which the glycoprotein gene (G) was deleted and replaced with genes encoding green fluorescent protein and luciferase. Wild-type spike was based on the Wuhan-Hu-1 sequence. Pseudoviruses were mixed with serial dilutions of ensovibep and pre-incubated for 90 min at 37°C before adding to pre-seeded VeroE6 cells. After 90 min incubation, the inoculum was removed, fresh medium was added, and cells were further incubated for 16 h. Cells were lysed according to the ONE-Glo™ luciferase assay system. Relative light units were measured and IC_{50} values were calculated using non-linear regression. Additional details can be found in Rothenberger et al 2022.
- Lentivirus pseudoviruses (ACTIV/FDA) bearing the spike proteins and carrying a firefly luciferase reporter gene were produced in 293T cells by co-transfection of pCMVDELR8.2, pHR'CMVLuc and pCDNA3.1(+)-spike variants. Wild-type spike was based on the Wuhan-Hu-1 sequence. Pseudoviruses were pre-incubated with serially diluted ensovibep for 2 h at 37°C before adding to pre-seeded 293T-ACE2.TMPRSS2s cells. Pseudovirus infection was scored 48 h later by measuring luciferase activity, and IC_{50}s were calculated using non-linear regression. Additional details can be found in Neerukonda et al 2021.
- Live authentic virus assay (Spiez Laboratory): Wild-type virus was a French isolate with the following changes compared with Wuhan-Hu-1: V367F, E990A. Serial dilutions of ensovibep were pre-incubated with 100 $TCID_{50}$ SARS-CoV-2 variants for 1 h at 37°C before adding to pre-seeded VeroE6-TMPRSS2 cells. After 3 day incubation, cell viability was measured using CellTiter-Glo. Luminescence was measured and IC_{50} values were calculated using non-linear regression. Additional details can be found in Rothenberger et al 2022.
- Live spike chimeric reporter viruses (UTMB) were constructed on the genetic background of an infectious cDNA clone derived from clinical strain WA1 (2019-nCoV/USA_WA1/2020) containing a mNeoGreen (mNG) reporter gene, and spike mutations were engineered using a PCR-based mutagenesis protocol. The full-length genomic cDNAs were in vitro ligated, transcribed, and electroporated into VeroE6 cells, and mutant viruses were recovered 3 days after electroporation. Mutant viruses were pre-incubated with serial dilutions of ensovibvep for 1 h at 37°C before adding to pre-seeded Vero E6-TMPRSS2 cells. After 1 h infection, the inoculum was removed and replaced with overlay medium (DMEM with 0.8% methylcellulose, 2% FBS, and 1% P/S). After 16 h, raw images of mNG fluorescent foci were acquired, foci were counted, and IC_{50}s were determined using non-linear regression. Additional details can be found in Zou et al 2022.

Results

- Notably, ensovibep potency (IC_{50}) against all tested variants remains in the range of 1-10 ng/mL; less than an order of magnitude difference from the reference/Wuhan WT virus (**Figure 3**) (Rothenberger et al 2022).

Figure 3. Ensovibep activity measured in neutralization assays performed with lentivirus, VSV-based pseudoviruses or authentic viruses for the SARS-CoV-2 variants of concern and variants of interest.

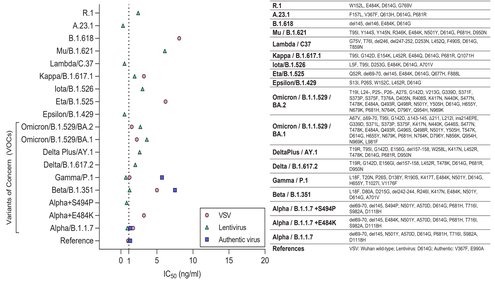

Variant	Substitutions / Deletions
R.1	W152L, E484K, D614G, Q769V
A.23.1	F157L, V367F, Q613H, D614G, P681R
B.1.618	del145, del146, E484K, D614G
Mu / B.1.621	T95I, Y144S, Y145N, R346K, E484K, N501Y, D614G, P681H, D950N
Lambda / C37	G75V, T76I, del246, del247-253, D253N, L452Q, F490S, D614G, T859N
Kappa / B.1.617.1	T95I, G142D, E154K, L452R, E484Q, D614G, P681R, Q1071H
Iota/B.1.526	L5F, T95I, D253G, E484K, D614G, A701V
Eta/B.1.525	Q52R, del69-70, del145, E484K, D614G, Q677H, F888L
Epsilon/B.1.429	S13I, P26S, W152C, L452R, D614G
Omicron / B.1.1.529 / BA.2	T19I, L24-, P25-, P26-, A27S, G142D, V213G, G339D, S371F, S373P, S375F, T376A, D405N, R408S, K417N, N440K, L452R, S477N, T478K, E484A, Q493R, Q498R, N501Y, Y505H, T547K, D614G, H655Y, N679K, P681H, N764K, D796Y, Q954H, N969K
Omicron / B.1.1.529 / BA.1	A67V, del69-70, del143-145, del211, L212I, G339D, S371F, S373P, S375F, T376A, D405N, K417N, N440K, G446S, S477N, T478K, E484A, Q493R, Q498R, N501Y, Y505H, T547K, D614G, H655Y, N679K, P681H, N764K, D796Y, Q954H, N969K, L981F
DeltaPlus / AY.1	T19R, T95I, G142D, E156G, del157-158, W258L, K417N, L452R, T478K, D614G, P681R, D950N
Delta / B.1.617.2	T19R, G142D, E156G, del157-158, L452R, T478K, D614G, P681R, D950N
Gamma / P.1	L18F, T20N, P26S, D138Y, R190S, K417T, E484K, N501Y, D614G, H655Y, T1027I, V1176F
Beta / B.1.351	L18F, D80A, D215G, del242-244, R246I, K417N, E484K, N501Y, D614G, A701V
Alpha / B.1.1.7 +S494P	del69-70, del144, S494P, N501Y, A570D, D614G, P681H, T716I, S982A, D1118H
Alpha / B.1.1.7 +E484K	del69-70, del145, E484K, N501Y, A570D, D614G, P681H, T716I, S982A, D1118H
Alpha / B.1.1.7	del69-70, del145, N501Y, A570D, D614G, P681H, T716I, S982A, D1118H
References	VSV: Wuhan wild-type; Lentivirus: D614G; Authentic: V367F, E990A

Reference variant is the Wuhan-Hu-1 strain for VSV-based pseudovirus, a D614G variant for the lentivirus-based pseudovirus or a patient isolate from the early pandemic for the authentic virus. VSV, vesicular stomatitis virus.

- Ensovibep was tested together with a panel of clinically relevant monoclonal antibodies (**Figure 4**).

Figure 4. Neutralization activities (titration curves and IC_{50}) of ensovibep and monoclonal antibodies.

Compound	Wild Type IC_{50} (ng/mL)	Omicron BA.1 IC_{50} (ng/mL)	Omicron BA.1 Fold change to WT
Ensovibep	1.6	2.2	1.4
REGN10933	3.2	>1000	>100
REGN10987	3.3	>1000	>100
LY-CoV555	13	>1000	>100
LY-CoV016	6.4	>1000	>100
S309	23	72	3.1
AZD8895	0.6	415	>100
AZD1061	5.5	237	43
Brii-196	9.5	392	41
Brii-198	52	30	0.6

IC_{50}: green: <10 ng/mL; orange: 10-100 ng/mL; dark orange: 100-1000 ng/mL; red: >1000 ng/mL Fold change to wt: green: <10-fold; orange: 10–100-fold; red: >100-fold

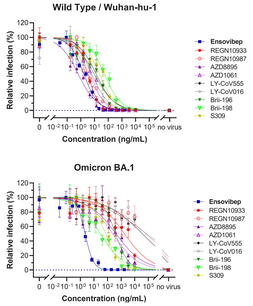

Titration curves (right panels; mean ±SEM) and IC_{50} values (above) for VSV-pseudotype neutralization assays with wild-type and Omicron BA.1 variant spike protein. Ensovibep was tested together with a panel of clinically validated monoclonal antibodies. The table provides the numeric IC_{50} values as well as the fold change with respect to the wild-type. Wild-type virus is Wuhan-Hu-1.

- A 10- to 40-fold increase in IC_{50} was seen for each indvidual DARPin (R1, R2, R3), however the multi-specific ensovibep containing all three RBD binding domains retained potency against BA.1 (**Figure 5**).

Figure 5. Titration curves and IC_{50} values of individual ensovibep DARPin modules against wild-type and BA.1 variant of SARS-CoV-2 in VSV-pseudotype neutralization assay.

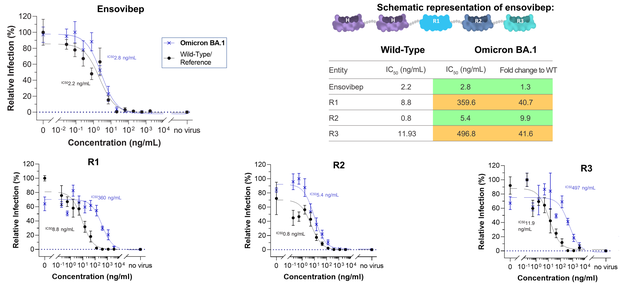

Entity	Wild-Type IC_{50} (ng/mL)	Omicron BA.1 IC_{50} (ng/mL)	Omicron BA.1 Fold change to WT
Ensovibep	2.2	2.8	1.3
R1	8.8	359.6	40.7
R2	0.8	5.4	9.9
R3	11.93	496.8	41.6

The table provides the numeric IC_{50} values as well as the fold change with respect to the wild-type. Wild-type virus is Wuhan-Hu-1.

- Ensovibep maintained its potency against omicron BA.2, as seen from the titration curves and IC_{50} values (**Figure 6**).

Figure 6. Ensovibep activity against SARS-CoV-2 wild-type (Wuhan-Hu-1) and omicron BA.2 variant in VSV-pseudotype neutralization assay.

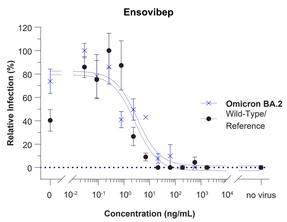

Entity	Wild-Type IC_{50} (ng/mL)	Omicron BA.2 IC_{50} (ng/mL)	Omicron BA.2 Fold change to WT
Ensovibep	2.8	3.3	1.2

(Above) Titration curves (above) and IC_{50} values (right) for ensovibep against SARS-CoV-2 WT and Omicron BA.2 variant showing potency is maintained against BA.2. (right) Table of the IC_{50} values and fold change.

The table provides the numeric IC_{50} values as well as the fold change with respect to the wild-type. Wild-type virus is Wuhan-Hu-1.

Figure 7. Ensovibep activity against wild-type and omicron variants using live spike chimeric reporter virus.

Variant	Spike mutations	IC_{50} (ng/mL)[a] Wild type	IC_{50} (ng/mL)[a] Variant	Fold change to Wild type
Delta / B.1.617.2	T19R, G142D, E156G, del157-158, L452R, T478K, D614G, P681R, D950N	3.8	3.0	0.8
Omicron / B.1.1.529 / BA.1	A67V, del69-70del, T95I, G142D, del143-145, del211, L212I, ins214EPE, G339D, S371L, S373P, S375F, K417N, N440K, G446S, S477N, T478K, E484A, Q493R, G496S, Q498R, N501Y, Y505H, T547K, D614G, H655Y, N679K, P681H, N764K, D796Y, N856K, Q954H, N969K, L981F	8.2	6.4	0.8
Omicron / B.1.1.529 / BA.2	T19I, del24-26, A27S, G142D, V213G, G339D, S371F, S373P, S375F, T376A, D405N, R408S, K417N, N440K, S477N, T478K, E484A, Q493R, Q498R, N501Y, Y505H, D614G, H655Y, N679K, P681H, N764K, D796Y, Q954H, N969K	3.8	12.1	3.2
Omicron / B.1.1.529 / BA.3	A67V, del69-70, T95I, G142D, del143-145, del211, L212I, G339D, S371F, S373P, S375F, D405N, K417N, N440K, G446S, S477N, T478K, E484A, Q493R, Q498R, N501Y, Y505H, D614G, H655Y, N679K, P681H, N764K, D796Y, Q954H, N969K	3.8	18.0	4.7
Omicron / B.1.1.529 / BA.2.12.1	T19I, del24-26, A27S, G142D, V213G, G339D, S371F, S373P, S375F, T376A, D405N, R408S, K417N, N440K, L452Q, S477N, T478K, E484A, Q493R, Q498R, N501Y, Y505H, D614G, H655Y, N679K, P681H, S704L, N764K, D796Y, Q954H, N969K	3.8[b]	9.6	2.5
Omicron / B.1.1.529 / BA.4/5[c]	T19I, del24-26, A27S, del69-70, G142D, V213G, G339D, S371F, S373P, S375F, T376A, D405N, R408S, K417N, N440K, L452R, S477N, T478K, E484A, F486V, Q498R, N501Y, Y505H, D614G, H655Y, N679K, P681H, N764K, D796Y, Q954H, N969K	3.8[b]	>10000	>2632

[a]IC_{50} values represent geometric means from 2–4 experiments. [b]Wild-type experiments were not conducted in parallel.[c]BA.4 and BA.5 share the same spike mutations. The table provides the numeric IC_{50} values as well as the fold change with respect to the Wild-type virus is Wuhan-Hu-1.

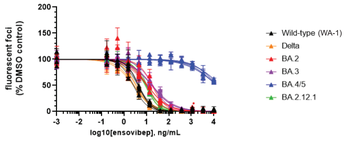

DMSO, Dimethyl sulfoxide

- BA.4 and BA.5 share the same spike sequence, so one experiment was performed to represent both viruses.
- Titration curves and IC_{50} values for ensovibep against SARS-CoV-2 wild-type (WA-1) and omicron BA.2, BA.3, BA.2.12.1, BA.4/5, and delta variants showing potency is maintained against all variants assessed with the exception of BA.4/5 (**Figure 7**).
- BA.4/5 sub-lineages of the omicron variant have a F486V mutation that reduces binding of the RBD binding DARPin domains, which is consistent with prior results from RBD mutational analysis in pseudovirus systems (**Figure 1**).

Conclusions

- The neutralization potency of ensovibep is maintained across SARS-CoV-2 variants, including BA.1, BA.2 and BA.2.12.1, and BA.3 of the omicron sub-lineages.
- A reduction in neutralization potency was observed with omicron sub-lineages BA.4/5, which is likely attributed to the F486V mutation present in this variant. The global incidences of BA.4 and BA.5 is low (<5%), with the exception of South Africa and Portugal. The potential for BA.4 and BA.5 to increase in incidence is currently unknown.
- These findings highlight the multi-specific and cooperative binding characteristics of ensovibep, which was designed with the intent to develop a durable treatment that could continue to bind to the spike protein of a rapidly evolving virus.
- Ensovibep continues to be investigated in clinical trials.

References

1. Rothenberger et al. 2022. Ensovibep, a novel trispecific DARPin candidate that protects against SARS-CoV-2 variants. BioRxiv. https://doi.org/10.1101/2021.02.03.429164.
2. Neerukonda et al. 2021. Establishment of a well-characterized SARS-CoV-2 lentiviral pseudovirus neutralization assay using 293T cells with stable expression of ACE2 and TMPRSS2. Plos One 16(3).
3. Zou et al. 2022. Neutralization against Omicron SARS-CoV-2 from previous non-Omicron infection. Nature Communications 13:852.

Acknowledgments

Independent support by investigators at the US Food and Drug Administration, Center for Biologics Evaluation and Research as part of Therapeutics Research Team for the US government COVID-19 response efforts.

The authors wish to thank Jing Zou, Xuping Xie, and Pei-Yong Shi in the Department of Biochemistry and Molecular Biology at the University of Texas Medical Branch, Galveston, TX, USA, and Stephanie Moquin, Mike Robinson, Johanne Blais, and Nadine Jarousse at the Novartis Institutes for BioMedical Research.

The authors were assisted in the preparation of the poster by Seónadh O'Leary and Rahul Lad (Novartis). The authors acknowledge Vajhula Sarma (Novartis) for designing the poster layout.

Poster presented at ASM Microbe June 9–13 in Washington D.C., USA.